

FUTURE B EXPERIMENTS FROM THE BTeV/LHC-B PERSPECTIVE

SHELDON STONE

Physics Department, Syracuse University, Syracuse N. Y., USA, 13244-1130
E-mail: stone@phy.syr.edu

Many measurements are necessary in the program of studying mixing, CP violation and rare decays of b and c quarks. These measurements require large numbers of B^0 , B_s , B^- and D^{*+} hadrons. Fortunately, copious production of particles containing b and c quarks will occur at Tevatron and the LHC. The crucial measurements are described here, as well as the design of the two experiments, LHC-b and BTeV, that can exploit the $4 - 20 \times 10^{11}$ b hadrons produced every 10^7 seconds.

1 Introduction

The basic experimental goals are to make exhaustive search for physics beyond the Standard Model and to precisely measure Standard Model parameters. I first discuss what studies need to be done, not just what studies can be done in the near future. Measurements are necessary on CP violation in B^0 and B_s mesons, B_s mixing, rare b decay rates, and mixing, CP violation and rare decays in the charm sector.

2 The CKM Matrix and CP Violation

2.1 The 6 Unitarity Triangles

The base states of quarks, the mass eigenstates, are mixed to form the weak eigenstates as described by the 3×3 complex Cabibbo-Kobayashi-Maskawa matrix,¹ that can be expressed in terms of 4 fundamental constants of nature, that need to be determined experimentally. In the Wolfenstein approximation² the matrix is written as:

$$\begin{pmatrix} 1 - \lambda^2/2 & \lambda & A\lambda^3(\rho - i\eta(1 - \lambda^2/2)) \\ -\lambda & 1 - \lambda^2/2 - i\eta A^2\lambda^4 & A\lambda^2(1 + i\eta\lambda^2) \\ A\lambda^3(1 - \rho - i\eta) & -A\lambda^2 & 1 \end{pmatrix}. \quad (1)$$

This expression is accurate to order λ^3 in the real part and λ^5 in the imaginary part. It is necessary to express the matrix to this order to have a complete formulation of the physics we wish to pursue.

Non-zero η allows for CP violation. CP violation thus far has only been seen in the neutral kaon system. By exploring CP violation in the b and c

systems we can see if the CKM model works or perhaps discover new physics that goes beyond the model, if it does not.

The unitarity of the CKM matrix allows us to construct six relationships. These equations may be thought of triangles in the complex plane. They are shown in Fig. 1.

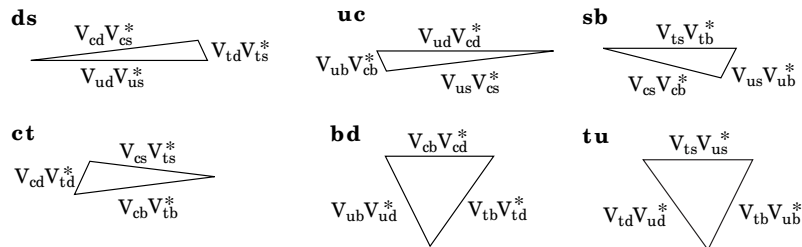


Figure 1. The six CKM triangles. The bold labels, e.g. **ds** refer to the rows or columns used in the unitarity relationship.

All six of these triangles can be constructed knowing four and only four independent angles.^{3,4,5} These are defined as:

$$\begin{aligned}
 \beta &= \arg \left(-\frac{V_{tb}V_{td}^*}{V_{cb}V_{cd}^*} \right), & \gamma &= \arg \left(-\frac{V_{ub}^*V_{ud}}{V_{cb}^*V_{cd}} \right), \\
 \chi &= \arg \left(-\frac{V_{cs}^*V_{cb}}{V_{ts}^*V_{tb}} \right), & \chi' &= \arg \left(-\frac{V_{ud}^*V_{us}}{V_{cd}^*V_{cs}} \right).
 \end{aligned}
 \tag{2}$$

Two of the phases β and γ are probably large while χ is estimated to be small ≈ 0.02 , but measurable, while χ' is likely to be much smaller.

In the **bd** triangle, the one usually considered, the angles are all thought to be relatively large. Since $V_{cd}^* = \lambda$, this triangle has sides 1 , $\frac{1}{\lambda} \left| \frac{V_{td}}{V_{ts}} \right|$, $\frac{1}{\lambda} \left| \frac{V_{ub}}{V_{cb}} \right|$. This CKM triangle is depicted in Fig. 2, with constraints from other measurements.⁶ Also shown are the angles α , β , and γ . Since they form a triangle the “real” α , β and γ must sum to 180° ; therefore measuring any two of these determines the third.

It has been pointed out by Silva and Wolfenstein³ that measuring these angles may not be sufficient to detect new physics. For example, suppose there is new physics that arises in $B^o - \bar{B}^o$ mixing. Let us assign a phase θ to this new physics. If we then measure CP violation in $B^o \rightarrow J/\psi K_S$ and eliminate any Penguin pollution problems in using $B^o \rightarrow \pi^+\pi^-$, then

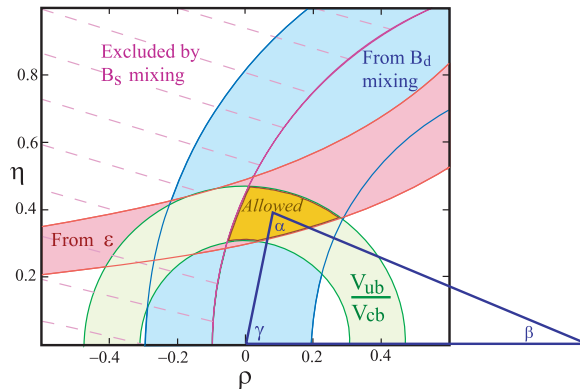


Figure 2. The CKM triangle shown in the $\rho - \eta$ plane. The shaded regions show $\pm 1\sigma$ contours given by $|V_{ub}/V_{cb}|$, neutral B mixing, and CP violation in K_L^0 decay (ϵ). The dashed region is excluded by B_s mixing limits. The allowed region is defined by the overlap of the 3 permitted areas, and is where the apex of the CKM triangle sits.

we actually measure $2\beta' = 2\beta + \theta$ and $2\alpha' = 2\alpha - \theta$. So while there is new physics, we miss it, because $2\beta' + 2\alpha' = 2\alpha + 2\beta$ and $\alpha' + \beta' + \gamma = 180^\circ$.

2.2 Ambiguities

In measuring CP phases there are always ambiguities. For example, any determination of $\sin(2\phi)$, has a four-fold ambiguity; $\phi, \pi/2 - \phi, \pi + \phi, 3\pi/2 - \phi$ are all allowed solutions. Often the point of view taken is that we know η is a positive quantity and thus we can eliminate two of the four possibilities. However, this is dangerous as it could lead to our missing new physics. Evidence that η is positive is derived from the measurements of ϵ and ϵ' using theoretical models. Even accepting that K_L decays give $\eta > 0$, it would be foolhardy to miss new physics just because we now assume that η must be positive rather than insisting on a clean measurement of the angles that could show a contradiction.

2.3 Technique for Measuring α

It is well known that $\sin(2\beta)$ can be measured without problems caused by Penguin processes using the reaction $B^0 \rightarrow J/\psi K_S$. The simplest reaction that can be used to measure $\sin(2\alpha)$ is $B^0 \rightarrow \pi^+\pi^-$. This reaction can proceed via both the Tree and Penguin diagrams shown in Fig. 3.

Current CLEO results⁸ are $\mathcal{B}(B^0 \rightarrow K^\mp \pi^\pm) = (1.88_{-0.26}^{+0.28} \pm 0.13) \times 10^{-5}$

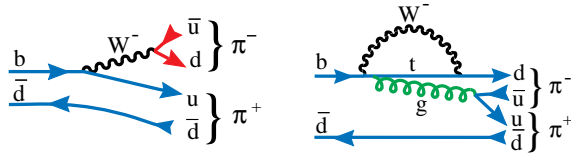


Figure 3. Processes for $B^0 \rightarrow \pi^+\pi^-$: Tree (left) and Penguin (right).

and $\mathcal{B}(B^0 \rightarrow \pi^+\pi^-) = (0.47_{-0.15}^{+0.18} \pm 0.06) \times 10^{-5}$, showing a relatively large Penguin amplitude that cannot be ignored. The Penguin contribution to $\pi^+\pi^-$ is roughly half the Tree *amplitude*. Thus the effect of the Penguin must be determined in order to extract α . The only model independent way of doing this was suggested by Gronau and London, but requires the measurement of $B^\mp \rightarrow \pi^\mp \pi^0$ and $B^0 \rightarrow \pi^0 \pi^0$, the latter being rather daunting.

There is however, a theoretically clean method to determine α . The interference between Tree and Penguin diagrams can be exploited by measuring the time dependent CP violating effects in the decays $B^0 \rightarrow \rho\pi \rightarrow \pi^+\pi^-\pi^0$ as shown by Snyder and Quinn.⁹

The $\rho\pi$ final state has many advantages. First of all, it has been seen with a relatively large rate. The branching ratio for the $\rho^0\pi^+$ final state as measured by CLEO¹⁰ is $(1.5 \pm 0.5 \pm 0.4) \times 10^{-5}$, and the rate for the neutral B final state $\rho^\pm\pi^\mp$ is $(3.5_{-1.0}^{+1.1} \pm 0.5) \times 10^{-5}$, while the $\rho^0\pi^0$ final state is limited at 90% confidence level to $< 5.1 \times 10^{-6}$. These measurements are consistent with some theoretical expectations.¹¹ Secondly, the associated vector-pseudoscalar Penguin decay modes have conquerable or smaller branching ratios. Furthermore, since the ρ is spin-1, the π spin-0 and the initial B also spinless, the ρ is fully polarized in the (1,0) configuration, so it decays as $\cos^2\theta$, where θ is the angle of one of the ρ decay products with the other π in the ρ rest frame. This causes the periphery of the Dalitz plot to be heavily populated, especially the corners. A sample Dalitz plot is shown in Fig. 4. This kind of distribution is good for maximizing the interferences, which helps minimize the error. Furthermore, little information is lost by excluding the Dalitz plot interior, a good way to reduce backgrounds.

To estimate the required number of events Snyder and Quinn preformed an idealized analysis that showed that a background-free, flavor-tagged sample of 1000 to 2000 events was sufficient. The 1000 event sample usually yields good results for α , but sometimes does not resolve the ambiguity. With the 2000 event sample, however, they always succeeded.

This technique not only finds $\sin(2\alpha)$, it also determines $\cos(2\alpha)$, thereby

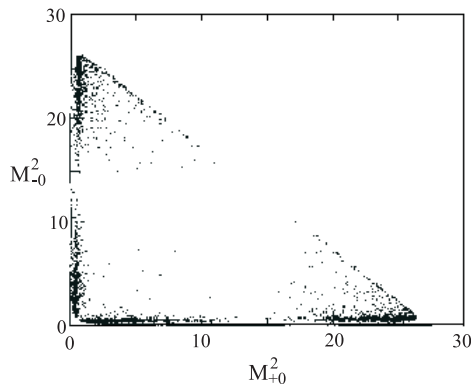


Figure 4. The Dalitz plot for $B^0 \rightarrow \rho\pi \rightarrow \pi^+\pi^-\pi^0$ from Snyder and Quinn.

removing two of the remaining ambiguities. The final ambiguity can be removed using the CP asymmetry in $B^0 \rightarrow \pi^+\pi^-$ and a theoretical assumption.¹²

2.4 Techniques for Measuring γ

In fact, it may be easier to measure γ than α . There have been at least four methods suggested.

(1) Time dependent flavor tagged analysis of $B_s \rightarrow D_s^\pm K^\mp$. This is a direct model independent measurement.¹³

(2) Measure the rate differences between $B^- \rightarrow \overline{D}^0 K^-$ and $B^+ \rightarrow D^0 K^+$ in two different D^0 decay modes such as $K^-\pi^+$ and K^+K^- . This method makes use of the interference between the tree and doubly-Cabibbo suppressed decays of the D^0 , and does not depend on any theoretical modeling.^{14,15}

(3) Rate measurements in two-body $B \rightarrow K\pi$ decays. A cottage industry has developed. However, all methods are model dependent.¹⁶

(4) Use U-spin symmetry to relate $B^0 \rightarrow \pi^+\pi^-$ and $B_s \rightarrow K^+K^-$.¹⁷

2.5 Required Measurements Involving β

The phase of $B^0 - \overline{B}^0$ mixing will soon be measured by e^+e^- b -factories using the $J/\psi K_S$ final state. New physics could be revealed by measuring other final states such as ϕK_S , $\eta' K_S$ or $J/\psi\pi^0$.

It is also important to resolve the ambiguities. There are two suggestions on how this may be accomplished. Kayser¹⁸ shows that time dependent

measurements of the final state $J/\psi K^o$, where $K^o \rightarrow \pi \ell \nu$, give a direct measurement of $\cos(2\beta)$ and can also be used for CPT tests. Another suggestion is to use the final state $J/\psi K^{*o}$, $K^{*o} \rightarrow K_S \pi^o$, and to compare with $B_s \rightarrow J/\psi \phi$ to extract the sign of the strong interaction phase shift assuming SU(3) symmetry, and thus determine $\cos(2\beta)$.¹⁹

2.6 A Critical Check Using χ

The angle χ , defined in equation 2, can be extracted by measuring the time dependent CP violating asymmetry in the reaction $B_s \rightarrow J/\psi \eta^{(\prime)}$, or if one's detector is incapable of quality photon detection, the $J/\psi \phi$ final state can be used. However, there are two vector particles in the final state, making this a state of mixed CP a requiring time-dependent angular analysis to find χ that requires large statistics.

Measurements of the magnitudes of CKM matrix elements all come with theoretical errors. Some of these are hard to estimate; we now try and view realistically how to combine CP violating phase measurements with the magnitude measurements to best test the Standard Model.

The best measured magnitude is that of $\lambda = |V_{us}/V_{ud}| = 0.2205 \pm 0.0018$. Silva and Wolfenstein^{3,4} show that the Standard Model can be checked in a profound manner by seeing if:

$$\sin \chi = \left| \frac{V_{us}}{V_{ud}} \right|^2 \frac{\sin \beta \sin \gamma}{\sin(\beta + \gamma)}. \quad (3)$$

Here the precision of the check will be limited initially by the measurement of $\sin \chi$, not of λ . This check can reveal new physics, even if other measurements have not shown any anomalies. There are other checks using $\left| \frac{V_{ub}}{V_{cb}} \right|$ or $\left| \frac{V_{td}}{V_{ts}} \right|$.⁶

2.7 Other Critical CKM Measurements and Summary

Magnitudes of the CKM elements are important to measure as precisely as possible. Current measurements of $|V_{cb}|$ and $|V_{ub}|$ are discussed elsewhere.²⁰

It has been predicted that $\Delta\Gamma/\Gamma$ for the B_s system is of the order of 10%. This can be determined by measuring the lifetimes in different final states such as $D_s^- \pi^+$ (mixed CP), $J/\psi \eta'$ (CP $-$) and $K^+ K^-$ (CP $+$). A finite $\Delta\Gamma$ would allow many other interesting measurements of CP violation.²¹

Table 1 lists the most important physics quantities and the suggested decay modes. The necessary detector capabilities include the ability to collect purely hadronic final states, the ability to identify charged hadrons, the ability to detect photons with good efficiency and resolution and excellent time

resolution required to analyze rapid B_s oscillations.

Table 1. Required CKM Measurements for b 's

Physics Quantity	Decay Mode	Hadron Trigger	$K\pi$ sep	γ det	Decay time σ
$\sin(2\alpha)$	$B^o \rightarrow \rho\pi \rightarrow \pi^+\pi^-\pi^o$	✓	✓	✓	
$\cos(2\alpha)$	$B^o \rightarrow \rho\pi \rightarrow \pi^+\pi^-\pi^o$	✓	✓	✓	
$\text{sign}(\sin(2\alpha))$	$B^o \rightarrow \rho\pi$ & $B^o \rightarrow \pi^+\pi^-$	✓	✓	✓	
$\sin(\gamma)$	$B_s \rightarrow D_s^\pm K^\mp$	✓	✓		✓
$\sin(\gamma)$	$B^- \rightarrow \overline{D}^0 K^-$	✓	✓		
$\sin(\gamma)$	$B^o \rightarrow \pi^+\pi^-$ & $B_s \rightarrow K^+K^-$	✓	✓		✓
$\sin(2\chi)$	$B_s \rightarrow J/\psi\eta', J/\psi\eta$			✓	✓
$\sin(2\beta)$	$B^o \rightarrow J/\psi K_s$				
$\cos(2\beta)$	$B^o \rightarrow J/\psi K^o, K^o \rightarrow \pi\ell\nu$				
$\cos(2\beta)$	$B^o \rightarrow J/\psi K^{*o}$ & $B_s \rightarrow J/\psi\phi$				✓
x_s	$B_s \rightarrow D_s^+\pi^-$	✓			✓
$\Delta\Gamma$ for B_s	$B_s \rightarrow J/\psi\eta', D_s^+\pi^-, K^+K^-$	✓	✓	✓	✓

3 Searches for New Physics

Because new physics at much larger mass scales can appear in loops, rare process such as $b \rightarrow s\gamma, d\gamma, sl^+\ell^-$ and $d\ell^+\ell^-$ have the promise to reveal new physics. Searches in both exclusive and inclusive final states are important.

Charm decays also offer the possibility of finding new physics in the study of either mixing or CP violation as the Standard Model prediction is small. The current experimental measurement of mixing is $r_D < 5 \times 10^{-3}$, while the SM expectation²² is $10^{-7} - 10^{-6}$. For CP violation the current limits are about 10%, while the expectation²³ is 10^{-3} .

4 The Next Generation of Experiments: LHC-b and BTeV

4.1 Rationale

To over constrain the CKM matrix and look for new physics, all the quantities listed in Table 1 must be measured. This requires large samples of b -flavored hadrons, and detectors capable of tolerating large interaction rates and having

excellent lifetime resolution, particle identification and γ/π^0 detection capabilities.

Fortunately, large samples of b quarks are available. With the Fermilab Main Injector, the Tevatron collider will produce $\approx 4 \times 10^{11}$ b hadrons/ 10^7 s at a luminosity of $2 \times 10^{32} \text{cm}^{-2} \text{s}^{-1}$. Rates are ≈ 5 times larger at the LHC. These compare very favorably to e^+e^- machines operating at the $\Upsilon(4S)$. At a luminosity of 3×10^{33} they produce 6×10^7 B 's/ 10^7 s. Furthermore B_s , Λ_b and other b -flavored hadrons are accessible for study at hadron colliders. Also important are the large charm rates, ~ 10 times larger than the b rate.

4.2 b Production Characteristics

Let us explore the reasons for the choice of the forward direction. It is often customary to characterize heavy quark production in hadron collisions with the two variables p_t and η , where $\eta = -\ln(\tan(\theta/2))$, and θ is the angle of the particle with respect to the beam direction. According to QCD based calculations of b quark production, the B 's are produced “uniformly” in η and have a truncated transverse momentum, p_t , spectrum characterized by a mean value approximately equal to the B mass.²⁴ The distribution in η is shown in Fig. 5. Note that at larger values of $|\eta|$, the B boost, $\beta\gamma$, increases rapidly.

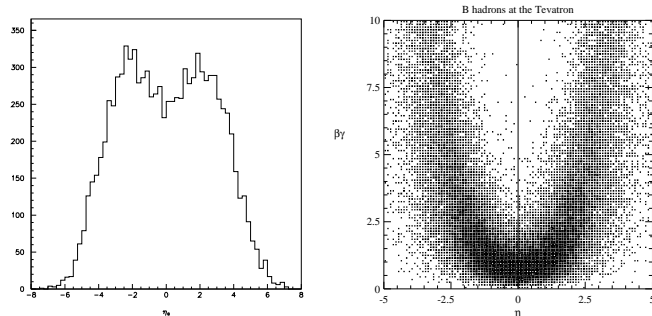


Figure 5. The B yield versus η (left). $\beta\gamma$ of the B versus η (right). Both plots are for the Tevatron.

The “flat” η distribution hides an important correlation of $b\bar{b}$ production at hadronic colliders. In Fig. 6 the production angles of the hadron containing the b quark is plotted versus the production angle of the hadron containing the \bar{b} quark according to the Pythia generator. Many important measurements require the reconstruction of a b decay and the determination of the flavor of the other \bar{b} , thus requiring both b 's to be observed in the detector. There

is a very strong correlation in the forward (and backward) direction: when the B is forward the \bar{B} is also forward. This correlation is not present in the central region (near zero degrees). By instrumenting a relative small region of angular phase space, a large number of $b\bar{b}$ pairs can be detected. Furthermore the B 's populating the forward and backward regions have large values of $\beta\gamma$.

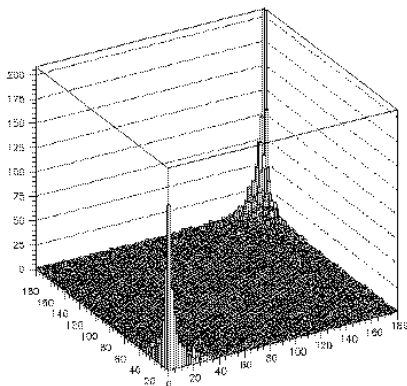


Figure 6. The production angle (in degrees) for the hadron containing a b quark plotted versus the production angle for a hadron containing \bar{b} quark. (For the Tevatron.) η of zero corresponds to 90° here.

Both experiments use forward spectrometers which utilizes the boost of the B 's at large rapidities. This is of crucial importance because the main way to distinguish b decays is by the separation of decay vertices from the main interaction vertex.

4.3 General Design Considerations

Two dedicated experiments are contemplated, LHC-b which has been approved and BTeV, an approved R&D program at Fermilab that was requested to prepare a proposal for submission in summer of 2000.²⁵ They both look for b decays in the “forward” direction close to the beam line to exploit the large b momenta and the correlated $b\bar{b}$ production. As a result, they both have long and narrow interaction regions. The C0 interaction region at Fermilab was constructed to allow the BTeV experiment to fit.

There are problems that heavy quark experiments at hadron colliders must overcome. First of all, the high b rate is accompanied by an even larger rate of uninteresting interactions. At the Tevatron the b -fraction is only 1/500, and is only 5 times larger at the LHC. In searching for rare processes, at the

level of parts per million, the background from b events is dominant. (Of course all b experiments have this problem.) The large data rate of b 's must be handled. For example, BTeV, has 1 kHz into the detector, and these events must be selected and written out. The electromagnetic calorimeter must be robust enough to deal with the particles from the underlying event and still have useful efficiency. Furthermore, radiation damage can destroy detector elements.

The strategy BTeV employs to overcome these obstacles includes triggering on events with detached vertices in the first trigger level. Both BTeV and LHC-b use the excellent detached vertex resolution, ~ 40 fs, to reject backgrounds in their analyses. Both experiments incorporate deadtimeless trigger and data acquisition systems, and have excellent Cherenkov Ring Imaging detectors to select charged hadrons. Furthermore BTeV has an excellent Electromagnetic calorimeter made from PbWO_4 crystals, based on the design of CMS. Both experiments can measure B_s mixing up to x_s values of 60-80.

LHC-b employs a somewhat different trigger strategy. They have a first level trigger (which they somewhat annoyingly call level-0) that selects events on the basis of having hadronic tracks or leptons with transverse momenta in the range of a few GeV/c. They then ask for detached vertices in the next trigger level.

4.4 Short Detector Descriptions

The LHC-b detector is shown in Fig. 7. The vertex detector is made from silicon strips. It is located in a magnetic field free region, and placed as close as 10 mm from the beam line. Two Ring Imaging Cherenkov detectors are used with different gases to cover the full momentum range for K/π separation. In addition, to separate kaons from protons, an aerogel radiator will likely be attached to the entrance window on the first RICH. There is a ‘‘Shaslik’’ style electromagnetic calorimeter made from scintillating fibers embedded in lead and a hadron calorimeter whose primary use is to veto crossing with more than one interactions, since these can confuse the trigger.

The BTeV Detector is shown in Fig. 8. It has two ‘‘forward’’ arms. This is done to increase the accepted b rate. BTeV must make up a factor of ≈ 5 to compete with LHC-b. BTeV has the vertex detector in the magnetic field. It is a pixel detector and is placed 6 mm from the beam line. BTeV believes that the detached vertex triggering is enhanced by eliminating low momentum, large multiple scattering tracks, from consideration. The single RICH, also with aerogel, is followed by a PbWO_4 electromagnetic calorimeter based on the design of CMS for radiation hard crystals. The crystals are

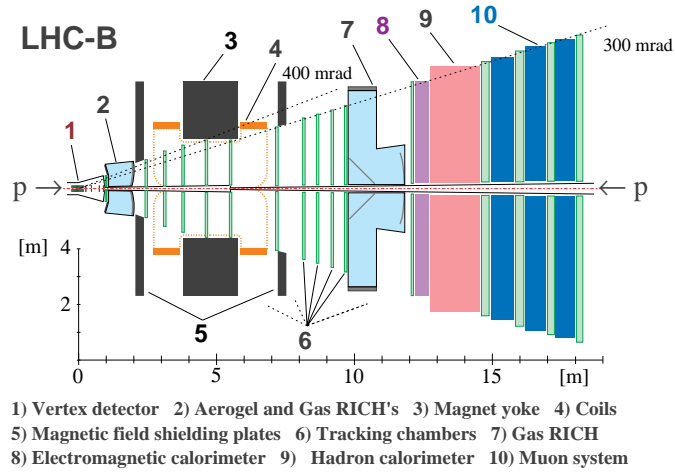


Figure 7. Schematic of the LHC-b detector.

approximately 26 mm x 26 mm x 220 mm. This gives good segmentation. Note that the lower momenta and multiplicities allow each arm of BTeV to be about half the length of LHC-b.

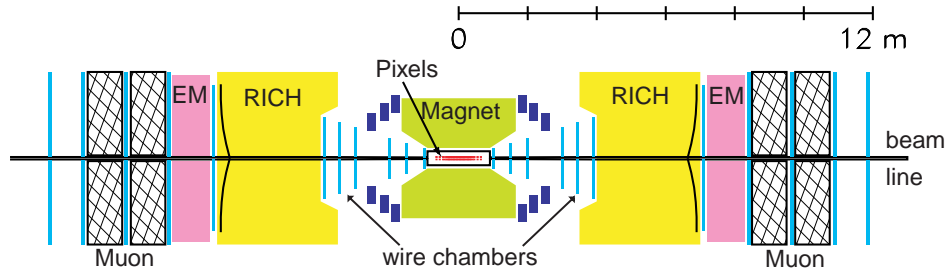


Figure 8. Schematic of the BTeV detector.

4.5 Some Sensitivity Projections

Space precludes a through discussion of sensitivities. I will discuss one illustrative example, the CP asymmetry in $B^0 \rightarrow \pi^+ \pi^-$. I use a BTeV simulation. The B^0 momentum distribution for events in the detector is shown in Fig. 9.

Also shown is the error in decay distance. The peak of the B^o momentum

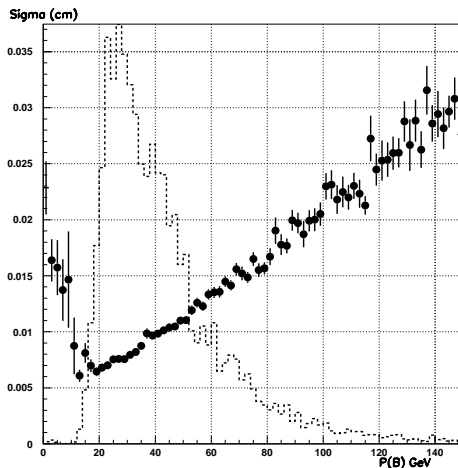


Figure 9. The momentum distribution (dashed) of B 's accepted by BTeV in the $\pi^+\pi^-$ decay mode along with the error on the vertex position measurement (solid points).

distribution is about 30 GeV/c. Since the average decay length goes as $480 \mu\text{m} \times p_B/m_B$, 30 GeV/c B 's go about 3 mm. Below about 20 GeV/c the error on measuring the decay distance grows, while above the decay distance error grows linearly with B momentum. The error growth at low momentum is due to multiple scattering. Since the key variable is decay distance divided by the error on decay distance, L/σ , it is best to have B 's above 20 GeV/c. L/σ is key in triggering as well as rejecting background. However, another significant source of background could be the other two-body decays into two pseudoscalars. These include $B^o \rightarrow K^\pm\pi^\mp$ and K^+K^- , and $B_s \rightarrow K^+K^-$ and $K^\pm\pi^\mp$. Fig. 10 shows the reconstructed mass spectra using the current CLEO measured branching ratios⁸ for $K^-\pi^+$ and $\pi^+\pi^-$, and assuming the corresponding modes in B_s decay have the same branching fractions. The $\pi^+\pi^-$ signal is completely swamped. However, the RICH particle identification should remove almost all the background. The relevant sensitivity calculations are shown for LHC-b and BTeV in Table 2

Comparing with e^+e^- machines at a luminosity of 3×10^{33} , the sensitivity is vastly greater; there are only 13 flavor tagged $\pi^+\pi^-$ events in e^+e^- .

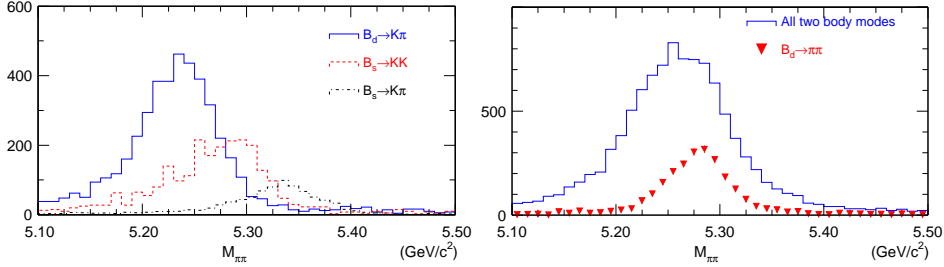


Figure 10. Two-body mass plots without particle identification left) $B_d \rightarrow K^+ \pi^-$, $B_s \rightarrow \pi^+ K^-$, $B_s \rightarrow K^+ K^-$, right) $B_d \rightarrow \pi^+ \pi^-$ and a sum of all two body decay modes. All particles are assumed to be pions.

Table 2. Sensitivity for the CP Asymmetry in $B^0 \rightarrow \pi^+ \pi^-$

Quantity	BTeV	LHC-b
b cross-section	100 μb	500 μb
Luminosity	$2 \times 10^{32} \text{cm}^{-2} \text{s}^{-1}$	$2 \times 10^{32} \text{cm}^{-2} \text{s}^{-1}$
# B^0 /Year (10^7 s)	1.4×10^{11}	7.0×10^{11}
$\mathcal{B}(B^0 \rightarrow \pi^+ \pi^-)$	0.47×10^{-6}	0.47×10^{-6}
Reconstruction efficiency	0.06	0.03
Triggering efficiency	0.50	0.17
# of $(\pi^+ \pi^-)$	20,000	18,700
ϵD^2 for flavor tags	0.1	0.1
Signal/Background	0.4	0.67
Error in Asymmetry	± 0.042	± 0.037

5 Conclusions

Both LHC-B and BTeV will be able to make what we now consider to be the quintessential measurements in b and charm physics. The sensitivities on the angle γ are estimated to be better than 10° . It is likely that at least two of the ambiguities in $\sin(2\beta)$ will be resolved. To measure α the reaction $B^0 \rightarrow \rho\pi$ looks most promising. Here preliminary estimates give BTeV a factor of 50 larger efficiency. However, neither experiment has estimated the backgrounds. Both experiments aim toward measuring χ . BTeV, with its excellent electromagnetic calorimeter will use primarily the $B_s \rightarrow J/\psi\eta'$ mode, while both experiments will also use the $J/\psi\phi$ final state. Besides the

precise measurement of CKM angles and resolving ambiguities, the search for new physics will be of paramount importance.

6 Acknowledgments

Support for this work was provided by the National Science Foundation. I thank George Hou and Hai-Yang Cheng for organizing an excellent and fruitful meeting. I thank Marina Artuso, Boris Kayser and Tomasz Skwarnicki for many useful discussions.

References

1. N. Cabibbo, *Phys. Rev. Lett.* **10**, 531 (1963); M. Kobayashi and K. Maskawa, *Prog. Theor. Phys.* **49**, 652 (1973).
2. L. Wolfenstein, *Phys. Rev. Lett.* **51**, 1945 (1983).
3. J. P. Silva, L. Wolfenstein, *Phys. Rev. D* **55**, 5331 (1997) [hep-ph/9610208].
4. R. Aleksan, B. Kayser and D. London, *Phys. Rev. Lett.* **73**, 18 (1994) [hep-ph/9403341].
5. I. I. Bigi and A. I. Sanda, “On the Other Five KM Triangles,” [hep-ph/9909479].
6. S. Stone, “Future of Heavy Flavour Physics: Experimental Perspective,” presented at Heavy Flavours 8, Southampton, UK, 1999, [hep-ph xxxx].
7. T. Blum *et al.*(RIKEN-BNL-Columbia), hep-lat/9908025.
8. Y. Kwon *et al.* (CLEO), “Study of Charmless Hadronic B Decays into the Final States $K\pi$, $\pi\pi$ and KK , with the First Observations of $B^0 \rightarrow \pi^+\pi^-$ and $B^0 \rightarrow K^0\pi^0$,” Conf 99-14, [hep-ex/9908039].
9. A. E. Snyder and H. R. Quinn, *Phys. Rev. D* **48**, 2139 (1993).
10. Y. Gao and F. Würthwein, CLEO preprint [hep-ex/9904008].
11. A. Ali, G. Kramer, and C.D. Lu, *Phys. Rev. D* **59**, 014005 (1999) [hep-ph/9805403].
12. Y. Grossman and H. R. Quinn, *Phys. Rev. D* **56**, 7259 (1997) [hep-ph/9705356].
13. D. Du, I. Dunietz and Dan-di Wu, *Phys. Rev D* **34**, 3414 (1986); R. Aleksan, I Dunietz, and B. Kayser, *Z. Phys. C* **54**, 653 (1992); R. Aleksan, A. Le Yaouanc, L. Oliver, O. Pène and J.-C. Raynal, *Z. Phys. C* **67** (1995) 251 [hep-ph/9407406].
14. D. Atwood, I. Dunietz and A. Soni, *Phys. Rev. Lett.* **78**, 3257 (1997).
15. M. Gronau and D. Wyler, *Phys. Lett. B* **265**, 172 (1991).

16. R. Fleischer, and T. Mannel, *Phys. Rev. D* **57**, 2752 (1998) [hep-ph/9704423]; M. Neubert and J. L. Rosner, *Phys. Rev. Lett.* **81**, 5076 (1998) [hep-ph/9809311]; M. Gronau, and J. L. Rosner, *Phys. Rev. D* **57**, 6843 (1998) [hep-ph/9711246]; M. Gronau, and D. Pirjol, [hep-ph/9902482]; M. Gronau and J. L. Rosner, *Phys. Rev. D* **59**, 113002 (1999) [hep-ph/9809384]; J.-M. Gerard and J. Weyers, *Eur. Phys. J C* **7**, 1 (1999) [hep-ph/9711469].
17. R. Fleischer, *Phys. Lett. B* **459**, 306 (1999) [hep-ph/9903456].
18. B. Kayser, “Cascade Mixing and the CP-Violating Angle Beta,” [hep-ph/9709382]. Previous work in this area was done by Y. Azimov, *Phys. Rev. D* **42**, 3705 (1990).
19. A. Dighe, I. Dunietz and R. Fleischer, *Phys. Lett. B* **433**, 147 (1998) [hep-ph/9804254].
20. Marina’s EPS
21. For a recent calculation of $\Delta\Gamma_s$, see M. Beneke, G. Buchalla, C. Greub, A. Lenz and U. Nierste, *Phys. Lett. B* **459**, 631 (1999) [hep-ph/9808385]. See also I. Dunietz, *Phys. Rev. D* **52**, 3048 (1995).
22. H. Georgi, *Phys. Lett. B* **297**, 353 (1992); T. Ohl *et al.*, *Nucl. Phys. B* **403**, 603 (1993).
23. F. Buccella *et al.*, *Phys. Lett. B* **302**, 319 (1993); F. Buccella *et al.*, *Phys. Lett. B* **379**, 249 (1996).
24. M. Artuso, “Experimental Facilities for b-Quark Physics,” in *B Decays* revised 2nd Edition, Ed. S. Stone, World Scientific, Sinagapore (1994).
25. Harnew has recently discussed the prospects for these experiments and CMS and ATLAS as well. See N. Harnew, “Prospects for LHC-b, BTeV, ATLAS, CMS,” in proceedings of HF8.